Studying an engineering model on an air blast wave

Z. Wang, X. Gong, J. Xiong & H. Yong
Institute of Applied Physics and Computational Mathematics, Beijing, China

Abstract

This paper presents a new engineering model on the air blast wave of TNT explosive. The model is built and the parameters are calibrated based on numerical simulated pressure time data of shock wave in air. The model describes the peak overpressure, impulse, typical time and attenuation coefficient of the shock wave with new computational equations. Comparison of pressure configuration for the scaled distance shows that the present engineering model can give consistent results with the numerical code and experiments.
Keywords: blast wave, overpressure, numerical simulation, engineering model.

1 Introduction

Impact loading of air blast is important in a variety of weapon design and the research of defending safeguard. The engineering computational model of air blast wave describes the rules of overpressure time with respect to the scaled distance after an explosion in air of equivalent TNT explosive. Based on analysis of experiments Friedlander [1] presented a strong practical model that the overpressure distribution in time at the positive phase zone is $\Delta p^{+}(t)=\Delta p_s\left(1-\overline{t}\right)e^{-\alpha\overline{t}}$, where Δp_s is peak overpressure, $\overline{t}$ is dimensionless time that determines the time when shock front arrives and the positive phase duration, α is the attenuation coefficient of overpressure. Δp_s, $\overline{t}$ and α are crucial in importance for describing overpressure distribution and many researchers persevered in improving the computational model of them [2–10]. As peak overpressure Δp_s, a lot of engineering equations have been presented based on experiments or numerical simulation [2–7]. Among them, Henrych [5] and Kinney and Grahma [6] showed consistent results with test data for nearly

WIT Transactions on The Built Environment, Vol 141, © 2014 WIT Press
www.witpress.com, ISSN 1743-3509 (on-line)
doi:10.2495/SUSI140191

all the range of the scaled distance. But $\bar{t}$ and α are closely related to evolution of overpressure and impulse of shock wave in air and they showed very complicated nonlinearly for different amount of explosive and scaled distance. So it is very difficult to determine widely adaptive equations for two of them just by analysis of experiments. Another problem is about the negative phase duration of air blast wave which is usually ignored in the previous studies but a number of researchers thought it is very important [8–10].

The motivation of the article is to build a new engineering computational model that can nicely describe air blast wave for a long range of the scaled distance. And the simple and practical equations are tried to be used for the model based on numerical simulated pressure time data. Some results of numerical simulation on explosion process of 1kg spherical TNT explosive are given firstly as the base of study, and then the computational approaches for the peak overpressure, minimum negative overpressure, impulse, typical time and attenuation coefficient are presented. After all the parameters are calibrated, some comparison of overpressure distribution shows that the present model gives consistent results with numerical code and experiments.

2 Numerical simulation results

A Lagrange code CHAP is used for numerical simulation on explosion process. The EOS for detonation products is Jones-Wilkins-Lee (JWL) as

$$P = \mathrm{A}\left(1-\frac{\omega}{\mathrm{R}_1\bar{v}}\right)\exp\left(-\mathrm{R}_1\bar{v}\right)+\mathrm{B}\left(1-\frac{\omega}{\mathrm{R}_2\bar{v}}\right)\exp\left(-\mathrm{R}_2\bar{v}\right)+\omega\frac{E}{\bar{v}} \tag{1}$$

where $\bar{v} = v/v_0$ is relative volume, E is internal energy per unit reference volume. The others parameters are A=373.77GPa, B=3.7471GPa, R_1=4.5, R_2=0.9, ω=0.35. The density of TNT is $\rho_{TNT}=1.63$ g/cm^3, the detonation speed is $D_{\mathrm{CJ}}=6.93$ km/s, the detonation pressure is $p_{\mathrm{CJ}}=21.0$ GPa, and the initial internal energy per unit reference volume $E_0=6.08$ GPa.

The ideal gas law is used for the EOS of air, including air density $\rho_0 = 1.225\ \mathrm{kg/cm^3}$, and ideal gas constant $\gamma = 1.4$.

A schematic of the blast wave based on numerical simulation with CHAP code is shown in Figure 1. The shock wave has an instantaneous rise and an exponential decay process. T_a, T_r, T_d and T_f are the shock wave front arrival time, the rising time for peak overpressure, the duration time for the positive overpressure and the final time that minimum negative overpressure can decrease to T_a is closely equal to T_r and the overpressure time history is usually assumed starting from the peak value and decreases exponentially, so T_a is ignored here just as in previous studies.

For a spherical free field explosion of 1kg TNT explosive, T_r, T_d, T_f, the peak overpressure Δp_s, the minimum negative overpressure Δp_f and the impulse of positive phase duration I^+ are shown in Table 1 with the distance from the explosion centre.

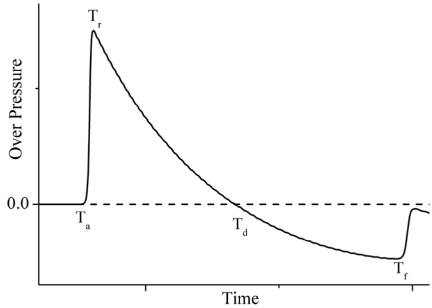

Figure 1: A schematic of the blast wave based on numerical simulation.

Table 1: Overpressure data with the explosion distance (1 kg spherical TNT).

R(m)	T_r(ms)	T_d(ms)	T_f(ms)	Δp_f (bar)	Δp_s (bar)	I^+ (Pa·s)
0.8	0.3610	0.9443	1.9584	0.3726	13.4027	145.4982
1.0	0.5479	1.2095	2.2323	0.3658	8.2580	112.8874
2.0	2.0734	3.3999	5.2379	0.2304	1.5617	67.3324
4.0	6.6863	8.9978	11.8155	0.1119	0.4049	37.4544
6.0	11.9571	14.7891	17.8966	0.0728	0.2107	25.3884
8.0	17.4536	20.6226	23.9346	0.0535	0.1376	19.1324
10.0	23.0598	26.4728	29.9331	0.0422	0.1005	15.3320
12.0	28.7281	32.3318	35.9059	0.0347	0.0784	12.7866
14.0	34.4375	38.1979	41.8715	0.0294	0.0639	10.9635
16.0	40.1745	44.0653	47.8310	0.0256	0.0536	9.5944
18.0	45.9316	49.9358	53.7762	0.0225	0.0461	8.5289
20.0	51.7962	55.7858	59.5719	0.0195	0.0383	7.6353
22.0	57.5850	61.6841	65.4859	0.0176	0.0340	6.9415
24.0	63.3894	67.5199	71.3843	0.0160	0.0305	6.3633
26.0	69.1940	73.4339	77.2515	0.0146	0.0276	5.8734
28.0	74.9985	79.2698	83.2751	0.0136	0.0251	5.4537
30.0	80.8187	85.1682	89.1266	0.0126	0.0231	5.0903
32.0	86.6389	91.0666	95.1189	0.0117	0.0213	4.7717
34.0	92.4748	96.8869	100.9704	0.0110	0.0198	4.4910
36.0	98.2950	102.7853	106.9471	0.0103	0.0185	4.2416
38.0	104.1309	108.6838	112.7674	0.0098	0.0173	4.0182
40.0	109.9668	114.5510	118.7441	0.0092	0.0163	3.8169
42.0	115.8183	120.4025	124.5643	0.0088	0.0153	3.6352
44.0	121.6542	126.2854	130.5254	0.0084	0.0145	3.4702

These data in Table 1 are the base of building the engineering blast model and calibrating parameters. As effected by the interface of detonation products, the schematic of the blast wave when R<0.8 m is different from Figure 1. Another note is that about 3000 other data are used for nicely analysis of peak overpressure Δp_s at the range of 0.07 <R<46.40 m.

3 Building engineering model

3.1 Overpressure and impulse

The scaled distance is $\overline{R} = R/\sqrt[3]{W}$, where R in m is the distance to explosion centre, W in kg is the mass of TNT explosive. The results of air blast wave are usually analyzed in double logarithmic diagrams in literature, so in this article the peak overpressure Δp_s is described as

$$lg\,\Delta p_s = \mathrm{a}\,\mathrm{e}^{-\mathrm{b}\overline{R}} - \mathrm{c}\,lg\,\overline{R} + \mathrm{d} \tag{2}$$

where a, b, c and d are parameters. When $\overline{R}$ gets large enough, Eqn (2) can be simplified to $lg\,\Delta p_s \approx -\mathrm{c}\,lg\,\overline{R} + \mathrm{d}$ which shows linearly relations in double logarithmic diagrams. An exponential decay item is added in Eqn (2) compared to overpressure model of Wu and Hao [7] at the large scaled distance.

Based on numerical simulation data, all the parameters are fitted and Δp_s in bar is determined as

$$\lg \Delta p_s = \begin{cases} 1.135\,\mathrm{e}^{-0.677\overline{R}} - 1.318\,\lg \overline{R} + 0.325, & 0.3 \le \overline{R} \le 46.4\ \mathrm{m}/\sqrt[3]{\mathrm{kg}} \\ -2.56\,\mathrm{e}^{-5.55\overline{R}} - 3.34\,\lg \overline{R} + 0.67, & \overline{R} < 0.3\ \mathrm{m}/\sqrt[3]{\mathrm{kg}} \end{cases} \tag{3}$$

Figure 2A shows the comparison of the peak overpressure results between numerical simulation and the fitted data and they agree very well. Figure 2B is relative error of fitted data for overpressure and it shows the maximum error is about 7%. Figure 3 is the comparison of the peak overpressure between the present model and the previous engineering equations [2–7] and some experiments in literature [11, 12].

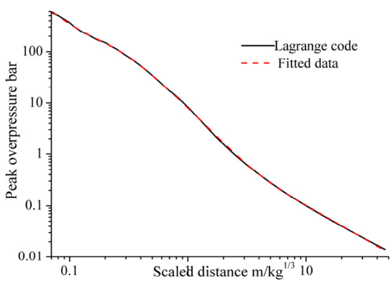

A: peak overpressure

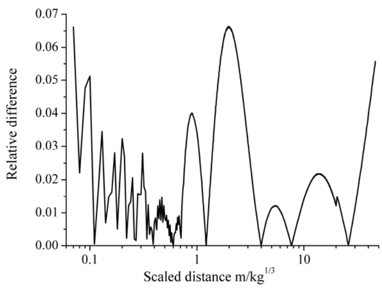

B: relative error of fitted data

Figure 2: Comparison of the peak overpressure.

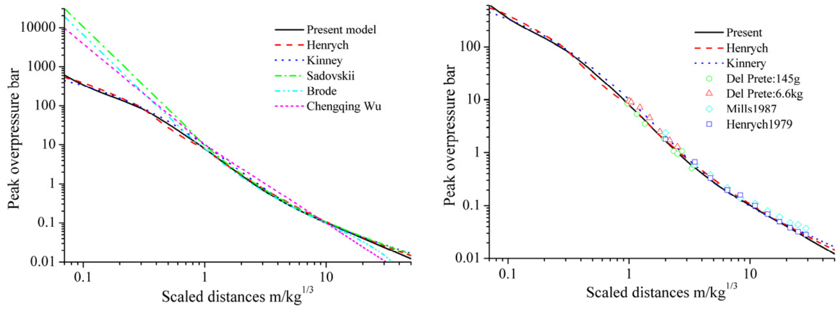

A: with engineering equations B: with test data in literature [11, 12]

Figure 3: Comparison of the peak overpressure.

Figure 3A shows that the present model gives consistent results with the equation of Henrych and Kinney and the other equations give greater overpressure when $\bar{R} \leq 1\,\mathrm{m}/\sqrt[3]{\mathrm{kg}}$. Some test data of the overpressure at the large scaled distance are added in Figure 3B.

Eqn (2) is also used to describe the minimum negative overpressure Δp_f and the positive phase impulse I^+ and after fitted data they are given as

$$\lg \Delta p_f = -1.98\,\mathrm{e}^{-2.67\bar{R}} - 1.08\ \lg \bar{R} - 0.3 \tag{4}$$

$$\lg I^+ = -0.24\,\mathrm{e}^{-0.7\bar{R}} - \lg \bar{R} + 2.186 \tag{5}$$

Eqn (5) is the impulse for 1 kg TNT, so it should be times $\sqrt[3]{W_{\mathrm{TNT}}}$ for the mass of TNT explosive W_{TNT}. Figures 4 and 5 show that the fitted results Δp_f and I^+ agree well with the numerical simulation data and they are linearly changed at a large scaled distance.

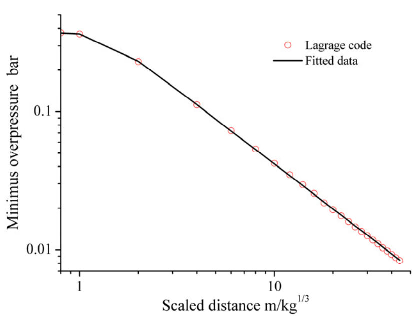

Figure 4: Comparison of Δp_f.

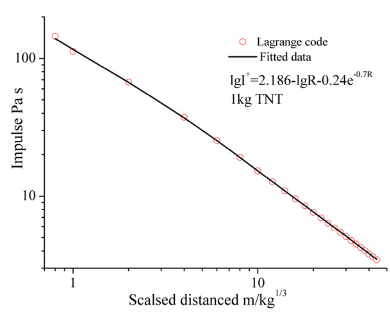

Figure 5: Comparison of I^+.

3.2 Typical time

The model of T_r, T_d and T_f need to be determined for building an engineering model for describing overpressure distribution such as Figure 1.

T_r can be computed by the relation of the shock front speed D_s with the peak pressure p_s in air as

$$D_s = \sqrt{\frac{(\gamma+1)p_s + (\gamma-1)p_0}{2\rho_0}} \tag{6}$$

where $p_s = \Delta p_s + p_0$, p_0 is the ambient pressure. So $T_r(R)$ can be derived by numerical integration as

$$T_r = T_0 + \int_{R_0}^{R} \frac{1}{D_s} dR = T_0 + \int_{R_0}^{R} \sqrt{\frac{2\rho_0}{(\gamma+1)p_s(R) + (\gamma-1)p_0}} dR \tag{7}$$

where R_0 is the radius of the spherical explosive, $T_0 = R_0 / D_{\mathrm{CJ}}$ is the time that the detonation wave gets to the outer boundary of the explosive. When $\gamma = 1.4$, Eqn (7) can be simplified to

$$T_r = T_0 + \int_{R_0}^{R} \sqrt{\frac{5\rho_0}{6p_s(R) + p_0}} dR \tag{8}$$

T_d and T_f are assumed to be given by

$$T_d = \left(1 + k_d / \overline{R}\right) T_r \tag{9}$$

$$T_f = \left(1 + k_f / \overline{R}\right) T_r \tag{10}$$

where k_d and k_f are parameters. By fitted data in Table 1, $k_f = 3.1$ is determined and from

$$\left(T_f - T_d\right) / \left(T_d - T_r\right) = k_f / k_d - 1 = \mathrm{f}\left(\overline{\mathrm{R}}\right) \tag{11}$$

k_d is determined by fitted model as

$$k_f / k_d - 1 = 0.93 + 0.89 \exp\left(-0.28 \overline{\mathrm{R}}\right) \tag{12}$$

Figure 6 is the results of $\mathrm{f}\left(\overline{\mathrm{R}}\right)$ from numerical simulation and Eqn (12). Figure 7 shows the comparison of the typical time T_r, T_d and T_f between numerical simulation and the present model and they agree well at a long range of scaled distance.

3.3 Attenuation coefficient of overpressure

When $T_r \le t \le T_d$, the overpressure model is described by Friedlander model as

$$\Delta p^+(t) = \Delta p_s \left(1 - \overline{t}\right) e^{-\alpha \overline{t}}, \quad \overline{t} = \left(t - T_r\right) / \left(T_d - T_r\right) \tag{13}$$

There are a lot of models such as Henrych [5], Wu and Hao [7] and Borgers and Vantomme [13] ($\alpha = 1.5\overline{R}^{-0.38}$) to determine the attenuation coefficient α. But we cannot obtain good results by using these models of α in the previous literature.

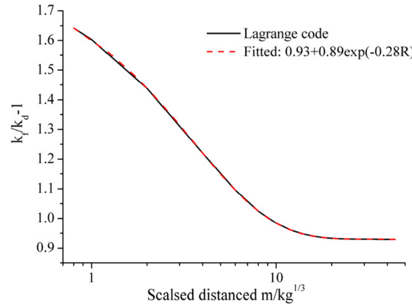

Figure 6: Results of $f(\bar{R})$.

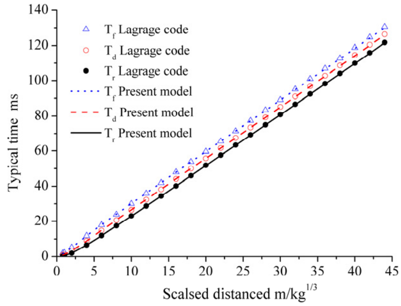

Figure 7: Results of typical time.

If α is not related to time, with Eqn (13) and $\int_{T_r}^{T_d} \Delta p^+(t)dt = I^+$, α can be determined as

$$\frac{\alpha^2}{\alpha - 1 + e^{-\alpha}} = \frac{\Delta p_s (T_d - T_r)}{I^+} \tag{14}$$

With the scaled distance increasing, the positive phase overpressure time distribution will be gradually close to a triangle curve, so α will gradually decrease to zero.

In the negative overpressure zone, when $T_d \le t$, Eqn (15) is used to describe the rule of overpressure and time.

$$\Delta p^-(t) = \Delta p^*(1 - \bar{t})\mathrm{e}^{-\beta(t)\bar{t}} \tag{15}$$

where $\beta(t)$ is the attenuation coefficient and it is related to time. Δp^* is parameter.

Here we note $\beta_d = \beta(T_d)$, $\beta_f = \beta(T_f)$, $\beta'_f = \beta'(T_f) = d\beta(t)/dt\big|_{t=T_f}$. For keeping the curve of overpressure time distribution continuity, with

$$d\Delta p^+(t)/dt\big|_{t=T_d} = d\Delta p^-(t)/dt\big|_{t=T_d} \tag{16}$$

We obtain

$$\Delta p_s \mathrm{e}^{-\alpha} = \Delta p^* \mathrm{e}^{-\beta_d} \tag{17}$$

With $\Delta p_f > 0$, note $\bar{t}_f = (T_f - T)_r / (T_d - T)_r$, and $\Delta p^-(T_f) = -\Delta p_f$ we obtain

$$\bar{t}_f \beta_f = \ln\left[\frac{\Delta p_s}{\Delta p_f}(\bar{t}_f - 1)\right] - \alpha + \beta_d \tag{18}$$

As

$$\frac{d\Delta p^-(t)}{dt} = -\frac{\Delta p^* e^{-\beta\bar{t}}}{(T_d - T_r)^2}\left[(T_d - T_r) - \beta(t - T_d) - \beta'(t - T_r)(t - T_d)\right] \tag{19}$$

Assuming $d\Delta p^-(t)/dt\big|_{t=T_f}=0$, we obtain

$$\beta_f\left(T_f-T_d\right)=\left(T_d-T_r\right)-\beta_f'\left(T_f-T_r\right)\left(T_f-T_d\right) \tag{20}$$

So β_d is the key value, if β_d is known, with Eqn (17), Eqn (18) and Eqn (20), Δp^*, β_f and β_f' can be separately determined. If set $\beta_d=\alpha$, then $\Delta p^*=\Delta p_s$, it is difficult to avoid $d^2\Delta p^-(t)/dt^2<0$ in $T_d\le t\le T_f$ at short scaled distance. Based on analysis of numerical simulation data and the character of Eqn (15), we set $\beta_f'\ge 0$ for $T_f\le t$ that means $\beta(t)$ will increase after that time and we obtain

$$\beta_d\le\frac{T_f-T_r}{T_f-T_d}+\alpha-\ln\left[\frac{\Delta p_s}{\Delta p_f}\left(\bar{t}_f-1\right)\right]=\beta_{d\max} \tag{21}$$

Then β_d is determined as $\beta_d=min\left(\alpha,\beta_{d\,max}\right)$.

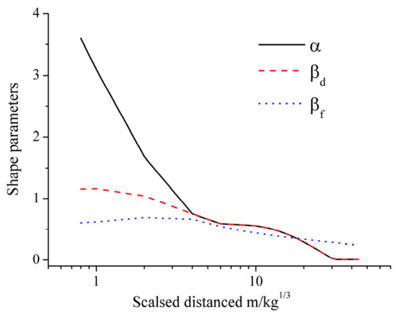

Figure 8: Typical value of attenuation coefficient.

Figure 8 gives the results of α, β_d and β_f changing with the scaled distance. Figure 8 shows that $\beta_d=\alpha$ is used when it is about $\overline{\mathrm{R}}>4\mathrm{m}/\sqrt[3]{\mathrm{kg}}$ and β_d is limited inside of this zone. When it is about $\overline{\mathrm{R}}>20\mathrm{m}/\sqrt[3]{\mathrm{kg}}$, $\beta_d>\beta_f$, but as $\beta_f'\ge 0$, $\beta(t)$ cannot be set as a simple linear decreasing model in $T_d\le t\le T_f$.

Based on analysis of β_d, β_f and β_f', the computational model of attenuation coefficient changing with time in the negative phase duration is assumed as

$$\beta(t)=\begin{cases}k_0+k_1t+k_2t^2, & T_d\le t\le T_f\\ \beta_f+\left(t-T_f\right)\beta_f', & T_f<t\end{cases} \tag{22}$$

where k_0, k_1 and k_2 are three parameters that can be determined from β_d, β_f

and β'_f, such as $k_2 = \beta'_f \big/ \left(T_f - T_d\right) - \left(\beta_f - \beta_d\right) \big/ \left(T_f - T_d\right)^2 \geq 0$, $k_1 = \beta'_f - 2k_2 T_f$, $k_0 = \beta_d - k_2 {T_d}^2 - k_1 T_d$. If $\beta_f \geq \beta_d$, set $k_2 = 0$, it is simple linear changing relation.

When the above models in the negative phase duration are being built, we always insist on two requirements, a) Trying to keep the curve of overpressure time distribution continuity, b) Trying to obtain agreeable results in the zone of $T_d \leq t \leq T_f$.

4 Results of the present model

Up to now, the whole engineering computational model of air blast wave is built and all the parameters can be determined. With a simple code of computing all equations, some results of the model are given by graphs comparing to the results of CHAP code and the results in literature.

Figure 9 shows results of overpressure time history. Good agreement is found between the numerical simulation and the present model. A, B and C in Figure 9 are results of 1kg TNT at the explosion distance of 1, 14 and 35m.

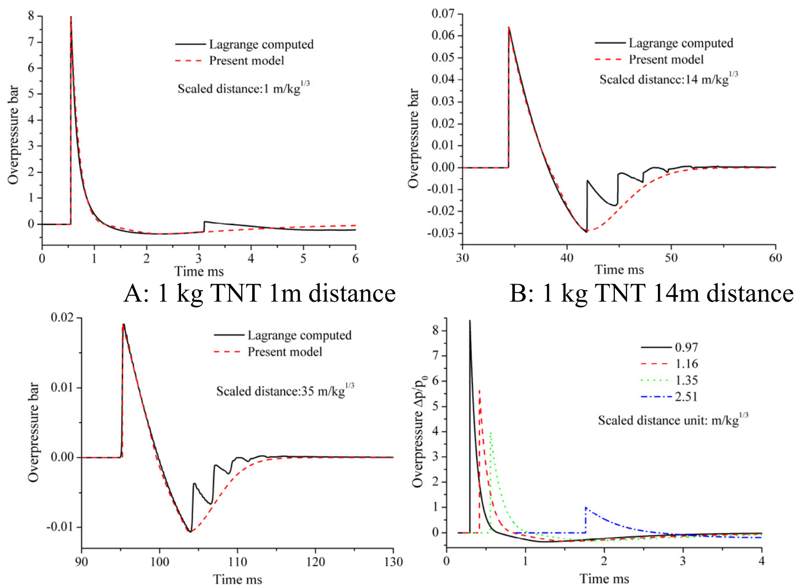

A: 1 kg TNT 1m distance   B: 1 kg TNT 14m distance

C: 1 kg TNT 35m distance   D: 0.18415 kg TNT

Figure 9: Overpressure time history.

Figure 9D shows the computed results of the present model for 0.18415kg TNT at 4 scaled distance as 0.97, 1.16, 1.35 and 2.51 $\mathrm{m}/\sqrt[3]{\mathrm{kg}}$. Comparing between results in Figure 9D and Figure 10 which is from literature [11], we can find that the overpressure time distribution are consistent.

www.witpress.com, ISSN 1743-3509 (on-line)

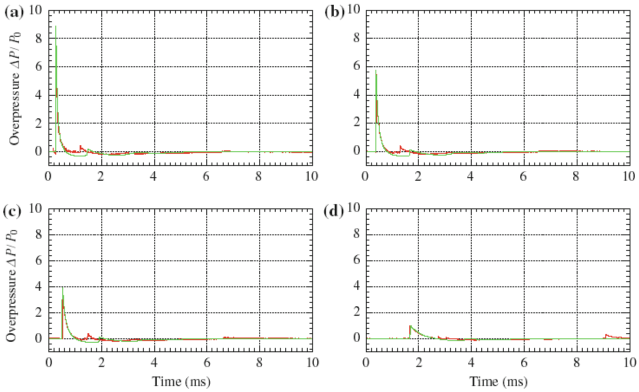

Figure 10: Results of the simulation and experiments in literature [11]. ((a) 0.97 $m/\sqrt[3]{kg}$, (b) 1.16 $m/\sqrt[3]{kg}$, (c) 1.35 $m/\sqrt[3]{kg}$, (d) 2.51 $m/\sqrt[3]{kg}$ 0.145kg PLANP explosive (0.18415 kg equivalent TNT).

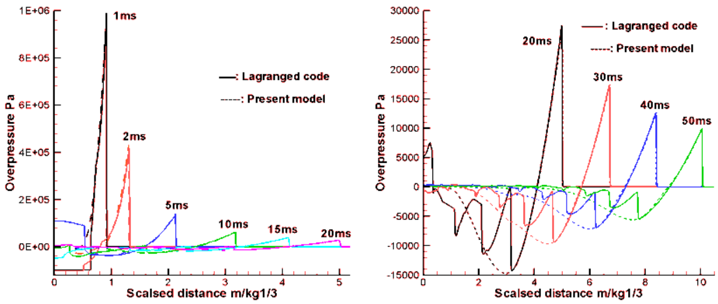

A: 1, 2, 5, 10, 15, 20ms B: 20, 30, 40, 50ms

Figure 11: Results of overpressure spatial distribution (1 kg TNT).

Figure 11 shows overpressure spatial distribution at different time for 1kg TNT explosive and the results between the present model and the numerical simulation agree very well.

5 Conclusion

Based on numerical simulated pressure time data, a new engineering computational model of air blast wave of TNT explosive is built and all the parameters can be determined by computing several equations. With the comparison and analysis of overpressure time or spatial distribution, it is showed that the present model can give consistent results with the numerical code and experiments and it can nicely describes air blast wave for a long range of scaled distance.

Acknowledgements

The work was performed under the auspices of NSFC (Grant No. 11371065). The additional support was provided by CAEP under project 2012A0202010.

References

[1] Friedlander FG, Note on the diffraction of blast waves by a wall. UK Home Office Dept, RC (A), 1939.

[2] Sadovskii MA, *Mechanical effects of air shock waves from explosion according to experiments*, Moscow: Izd Akad Nauk SSSR, 1952.

[3] Brode HL, Blast Wave from a Spherical Charge. *Phys Fluids*, 2, 2–17, 1959.

[4] Baker, WE, Cox, PA, Westine, PS, *Explosion hazards and evaluations*, Elsevier, 1983.

[5] Henrych J, *The Dynamics of Explosion and its Use*, Amsterdam: Elsevier, 1979.

[6] Kinney GF, Grahma KJ, *Explosive shocks in air,* New York: Springer, 1985.

[7] Chengqing Wu, Hong Hao, Modeling of simultaneous ground shock and airblast pressure on nearby structures from surface explosions. *International Journal of Impact Engineering,* 31, 699–717, 2005.

[8] Krauthammer T, Altenberg A, Negative phase blast effects on glass panels. *International Journal of Impact Engineering,* 24, 1–17, 2000.

[9] Wei J, Mahesh SS, Lokeswarappa RD, Dharani R, Failure analysis of architectural glazing subjected to blast loading. *Engineering Failure Analysis.* 13, 1029–1043, 2006.

[10] Teich M, Warnstedt P, Gebbeken N, The influence of negative phase loading on cable net facade response. *Journal of Architectural Engineering*, 18(4), 276–284, 2012.

[11] E·Del Prete, A·Chinnayya, L·Domergue, A·Hadjadj, JF Haas, Blast wave mitigation by dry aqueous foams. *Shock Waves*, 23, 39–53, 2013.

[12] Adel M·Benselama, Mame JP William Louis, François Monnoyer, A 1D–3D mixed method for the numerical simulation of blast waves in confined geometries. *Journal of Computational Physics,* 228, 6796–6810, 2009.

[13] Borgers JBW, Vantomme J, Towards a parametric model of a planar blast wave created with detonating cord. *Proc. of the 19th international symposium on the military aspects of blast and shock*, Calgary, Canada; 2006.

www.witpress.com, ISSN 1743-3509 (on-line)